

The Tale of H_0 Crisis and the Gravitational Transition

George Alestas

Theoretical Physics Section, Department of Physics, University of Ioannina

Supervisor: Prof. L. Perivolaropoulos

Based on

Phys.Rev.D 103 (2021) 8, 083517, by G. Alestas, L. Kazantzidis and L. Perivolaropoulos

Mon.Not.Roy.Astron.Soc. 504 (2021) 3956, by G. Alestas and L. Perivolaropoulos

ArXiv:2104.14481 [astro-ph.CO], by G. Alestas, I. Antoniou and L. Perivolaropoulos

The presentation slides can be found at <https://cosmology.physics.uoi.gr/seminars>

June 3, 2021



Overview

- 1 A General Introduction to the Crisis
- 2 A Late Time $w - M$ Transition Model as a Solution
- 3 Observational Evidence for a Gravitational Transition
- 4 Summary and Conclusions

What is the H_0 crisis?

- We consider the 2 basic methods of measuring the present value of $H(z)$:
 - 1 Using Cosmic Microwave Background (CMB) and Baryon Acoustic Oscillation (BAO) data.
 - 2 Using standard candles meaning SniIa calibrated with Cepheids (SH0ES), Red Giant stars or megamasers in accretion disks.

What is the H_0 crisis?

- We consider the 2 basic methods of measuring the present value of $H(z)$:
 - 1 Using Cosmic Microwave Background (CMB) and Baryon Acoustic Oscillation (BAO) data.
 - 2 Using standard candles meaning SnIa calibrated with Cepheids (SH0ES), Red Giant stars or megamasers in accretion disks.
- The first method produces,

$$H_0^{P18} = 67.36 \pm 0.54 \text{ km s}^{-1} \text{ Mpc}^{-1} \quad (1)$$

What is the H_0 crisis?

- We consider the 2 basic methods of measuring the present value of $H(z)$:
 - 1 Using Cosmic Microwave Background (CMB) and Baryon Acoustic Oscillation (BAO) data.
 - 2 Using standard candles meaning SniIa calibrated with Cepheids (SH0ES), Red Giant stars or megamasers in accretion disks.
- The first method produces,

$$H_0^{P18} = 67.36 \pm 0.54 \text{ km s}^{-1} \text{ Mpc}^{-1} \quad (1)$$

- While the second gives,

$$H_0^{R20} = 73.2 \pm 1.3 \text{ km s}^{-1} \text{ Mpc}^{-1} \quad (2)$$

N. Aghanim et al. (Planck), *Astron. Astrophys.* 641, A6 (2020), arXiv:1807.06209 [astro-ph.CO]

A. G. Riess, S. Casertano, W. Yuan, J. B. Bowers, L. Macri, J. C. Zinn, and D. Scolnic, (2020), arXiv:2012.08534 [astro-ph.CO]

H_0 or M_B Crisis?

H_0 crisis might not be such an accurate term after all...

- The truth is that the tension has very little to do with H_0 itself.

H_0 or M_B Crisis?

H_0 crisis might not be such an accurate term after all...

- The truth is that the tension has very little to do with H_0 itself.
- The true culprit is M_B , the SNeIa absolute peak magnitude.

H_0 or M_B Crisis?

H_0 crisis might not be such an accurate term after all...

- The truth is that the tension has very little to do with H_0 itself.
- The true culprit is M_B , the SNela absolute peak magnitude.
- The H_0 value given by the SH0ES distance ladder measurement is calculated indirectly by considering an inferred value of M_B from the Cepheid period-luminosity relation.

H_0 or M_B Crisis?

H_0 crisis might not be such an accurate term after all...

- The truth is that the tension has very little to do with H_0 itself.
- The true culprit is M_B , the SNela absolute peak magnitude.
- The H_0 value given by the SH0ES distance ladder measurement is calculated indirectly by considering an inferred value of M_B from the Cepheid period-luminosity relation.
- The problem is that that value of M_B was calculated for the redshift range $0.023 < z < 0.15$, therefore the H_0 value one gets from this method is a product of extrapolation.

Adam G. Riess et al., *Astrophys. J.* 699, 539–563 (2009), [arXiv:0905.0695 \[astro-ph.CO\]](https://arxiv.org/abs/0905.0695)

H_0 or M_B Crisis?

- More specifically a SH0ES-like value of H_0 can be given by,

$$\alpha_B = \left(\sum_{ij} C_{ij}^{-1} (\log_{10} \hat{d}_L(z) - 0.2m_B(i)) \right) / \sum_{ij} C_{ij}^{-1} \quad (3)$$

$$H_0 = 10^{0.2(M_B + 5a_B + 25)} \quad (4)$$

where C is the covariance matrix of the Pantheon SN magnitudes and the sums in Eq. (3) extend all SN in the Pantheon sample with redshifts in the range 0.023 – 0.15.

H_0 or M_B Crisis?

- More specifically a SH0ES-like value of H_0 can be given by,

$$\alpha_B = \left(\sum_{ij} C_{ij}^{-1} (\log_{10} \hat{d}_L(z) - 0.2m_B(i)) \right) / \sum_{ij} C_{ij}^{-1} \quad (3)$$

$$H_0 = 10^{0.2(M_B + 5a_B + 25)} \quad (4)$$

where C is the covariance matrix of the Pantheon SN magnitudes and the sums in Eq. (3) extend all SN in the Pantheon sample with redshifts in the range 0.023 – 0.15.

- This methodology is oblivious to any change below $z = 0.023$.

G. Efstathiou, (2021), [arXiv:2103.08723](https://arxiv.org/abs/2103.08723) [astro-ph.CO]

Do's and Don'ts regarding the tension

- Consider all available data (CMB, BAO, Snela, *etc.*).

Do's and Don'ts regarding the tension

- Consider all available data (CMB, BAO, Snela, *etc.*).
- Try to ease the growth tension as well, two birds one stone.

Do's and Don'ts regarding the tension

- Consider all available data (CMB, BAO, Snela, *etc.*).
- Try to ease the growth tension as well, two birds one stone.
- Do NOT use a local H_0 prior.

Do's and Don'ts regarding the tension

- Consider all available data (CMB, BAO, Snela, *etc.*).
- Try to ease the growth tension as well, two birds one stone.
- Do NOT use a local H_0 prior.
- If a prior is necessary make it an M prior instead.

The Two Paths to Follow

There are two schools of thought regarding this tension.

- The problem stems from systematic errors in the SH0ES calculations (e.g. Cepheid color-luminosity calibration systematics).

The Two Paths to Follow

There are two schools of thought regarding this tension.

- The problem stems from systematic errors in the SH0ES calculations (e.g. Cepheid color-luminosity calibration systematics).
- It is a gateway to new and exciting late and/or early time physics.

The Two Paths to Follow

There are two schools of thought regarding this tension.

- The problem stems from systematic errors in the SH0ES calculations (e.g. Cepheid color-luminosity calibration systematics).
- It is a gateway to new and exciting late and/or early time physics.

We will take the second (and most interesting) path, and more specifically we will consider a late time solution to the tension.

The Two Paths to Follow

There are two schools of thought regarding this tension.

- The problem stems from systematic errors in the SH0ES calculations (e.g. Cepheid color-luminosity calibration systematics).
- It is a gateway to new and exciting late and/or early time physics.

We will take the second (and most interesting) path, and more specifically we will consider a late time solution to the tension.

- We will consider a parametrization with a dark energy transition at very low redshifts ($z < 0.023$), coupled with a gravitational transition of about 10%.

E. Mortsell et al., (2021), [arXiv:2105.11461](https://arxiv.org/abs/2105.11461) [astro-ph.CO]

Motivation

It seems quite clear that new late time physics are needed in order to resolve the tension.

Motivation

It seems quite clear that new late time physics are needed in order to resolve the tension.

Due to nature of the problem, a simple dark energy transition even though it allows H_0 to approach the value reported by SH0ES, fails to solve the problem by itself.

Motivation

It seems quite clear that new late time physics are needed in order to resolve the tension.

Due to nature of the problem, a simple dark energy transition even though it allows H_0 to approach the value reported by SH0ES, fails to solve the problem by itself.

Another type of modification is needed. A gravitational transition which will in turn allow for a transition in M , the heart of the issue!

G. Alestas et al, Phys.Rev. D 99 064026 (2019)

Questions to address

- Is the proposed model able to provide a satisfying resolution to the Hubble crisis, without worsening the growth tension?

Questions to address

- Is the proposed model able to provide a satisfying resolution to the Hubble crisis, without worsening the growth tension?
- Is there any observational evidence for such a parametrization?

Defining the model

- We propose a parametrization which contains a transition of the SNIa absolute magnitude M at $z_t \in [0.01, 0.1]$ accompanied by transition of the equation dark energy of state parameter $w(z)$ (LwMPT).

Defining the model

- We propose a parametrization which contains a transition of the Smla absolute magnitude M at $z_t \in [0.01, 0.1]$ accompanied by transition of the equation dark energy of state parameter $w(z)$ (LwMPT).
- In particular, we consider a transition of $w(z)$ as,

$$w(z) = -1 + \Delta w \Theta(z_t - z) \quad (5)$$

coupled with a transition of the Smla absolute magnitude M of the form,

$$M(z) = M_C + \Delta M \Theta(z - z_t) \quad (6)$$

where Θ is the Heaviside step function, $M_C = -19.24$ is the Smla absolute magnitude calibrated by Cepheids at $z < 0.01$ and ΔM , Δw are parameters to be fit by the data.

G. Alestas et.al., *Phys.Rev.D* 103 (2021) 8, 083517

Camarena, David and Marra, Valerio, *Phys.Rev.Res.* 2 (2020) 1, 013028

Defining the model

- The evolution of dark energy density is

$$\rho_{de}(z) = \rho_{de}(z_p) \int_{z_p}^z \frac{dz'}{1+z'} (1+w(z')) = \rho_{de}(z_p) \left(\frac{1+z}{1+z_p} \right)^{3(1+w)} \quad (7)$$

where in the last equality a constant w was assumed and z_p is a pivot redshift which may be assumed equal to the present time or equal to the transition time z_t .

- And the Hubble expansion rate $h(z) \equiv H(z)/100\text{km}/(\text{sec} \cdot \text{Mpc})$ takes the form

$$h_w(z)^2 \equiv \omega_m(1+z)^3 + \omega_r(1+z)^4 + (h^2 - \omega_m - \omega_r) \left(\frac{1+z}{1+z_t} \right)^{3\Delta w} \quad z < z_t$$

$$h_w(z)^2 \equiv \omega_m(1+z)^3 + \omega_r(1+z)^4 + (h^2 - \omega_m - \omega_r) \quad z > z_t \quad (8)$$

Two important conditions to follow

We impose two conditions on the ansatz:

- It should reproduce the comoving distance corresponding to Planck18/ Λ CDM r_Λ for $z \gg z_t$ where

$$r_\Lambda(z) \equiv \int_0^z \frac{dz'}{\omega_m(1+z')^3 + \omega_r(1+z')^4 + (h^2 - \omega_m - \omega_r)} \quad (9)$$

where $\omega_m \equiv \Omega_{0m}h^2 = 0.143$, $\omega_r \equiv \Omega_{0r}h^2 = 4.64 \times 10^{-5}$ and $h = h_{CMB} = 0.674$.

- It should reproduce the local measurements of the Hubble parameter

$$h_w(z=0) = h_{local} = 0.74 \quad (10)$$

Two important conditions to follow

- The first condition fixes the parameters ω_m , ω_r and h to their Planck18/ Λ CDM best fit values.

Two important conditions to follow

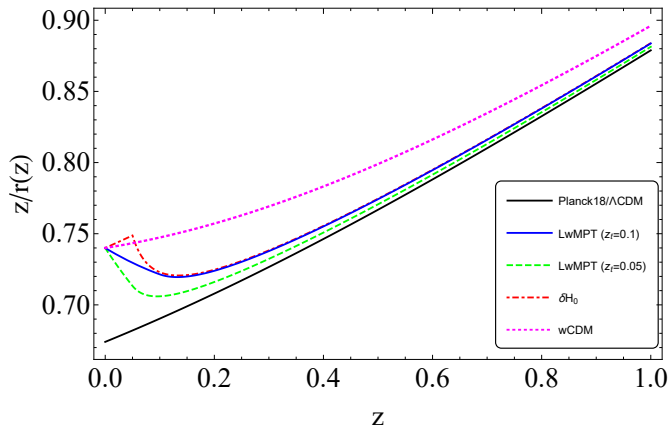
- The first condition fixes the parameters ω_m , ω_r and h to their Planck18/ Λ CDM best fit values.
- The second condition leads to a relation between Δw and z_t of the form,

$$\Delta w = \frac{\text{Log}(h^2 - \omega_m) - \text{Log}(h_{local}^2 - \omega_m)}{3\text{Log}(1 + z_t)} \quad (11)$$

where $h = h_{CMB} = 0.674$ and $\omega_m = \Omega_{0m}h^2 = 0.143$ as implied by the first condition and for consistency with the CMB anisotropy spectrum.

Comparing comoving distance forms

We compare the form of the comoving distance $r(z)$ predicted in the context of the $LwMPT$ model $r_w(z)$ with other proposed $H(z)$ deformations for the resolution of the Hubble tension that produce the same CMB anisotropy spectrum as Planck18/ Λ CDM while at the same time predict a Hubble parameter equal to its locally measured value $h(z=0) = h_{local}$.



Fitting LwMPT to cosmological data

We use the following datasets in order to fit the LwMPT, w CDM and Λ CDM models,

Fitting LwMPT to cosmological data

We use the following datasets in order to fit the LwMPT, w CDM and Λ CDM models,

- The Pantheon S_{nl}a dataset consisting of 1048 distance modulus datapoints in the redshift range $z \in [0.01, 2.3]$.

Fitting LwMPT to cosmological data

We use the following datasets in order to fit the LwMPT, w CDM and Λ CDM models,

- The Pantheon S_{nl}a dataset consisting of 1048 distance modulus datapoints in the redshift range $z \in [0.01, 2.3]$.
- A compilation of 9 BAO datapoints in the redshift range $z \in [0.1, 2.34]$.

Fitting LwMPT to cosmological data

We use the following datasets in order to fit the LwMPT, w CDM and Λ CDM models,

- The Pantheon S_{nl}a dataset consisting of 1048 distance modulus datapoints in the redshift range $z \in [0.01, 2.3]$.
- A compilation of 9 BAO datapoints in the redshift range $z \in [0.1, 2.34]$.
- The latest Planck18/ Λ CDM CMB distance prior data (shift parameter R and the acoustic scale l_a). These are highly constraining datapoints based on the observation of the sound horizon standard ruler at the last scattering surface $z \simeq 1100$.

Fitting LwMPT to cosmological data

We use the following datasets in order to fit the LwMPT, w CDM and Λ CDM models,

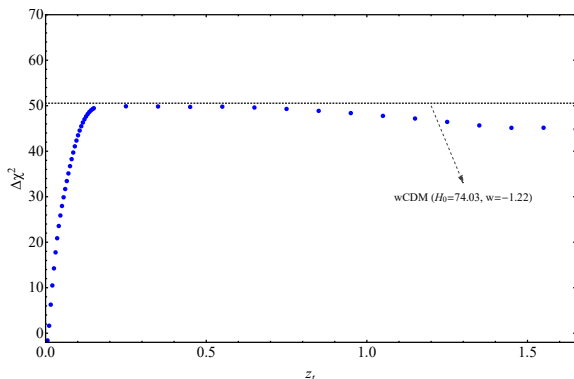
- The Pantheon S_{nl}a dataset consisting of 1048 distance modulus datapoints in the redshift range $z \in [0.01, 2.3]$.
- A compilation of 9 BAO datapoints in the redshift range $z \in [0.1, 2.34]$.
- The latest Planck18/ Λ CDM CMB distance prior data (shift parameter R and the acoustic scale l_a). These are highly constraining datapoints based on the observation of the sound horizon standard ruler at the last scattering surface $z \simeq 1100$.
- A compilation of 41 Cosmic Chronometer (CC) datapoints in the redshift range $z \in [0.1, 2.36]$.

Fitting LwMPT to cosmological data

- We therefore define χ^2 as

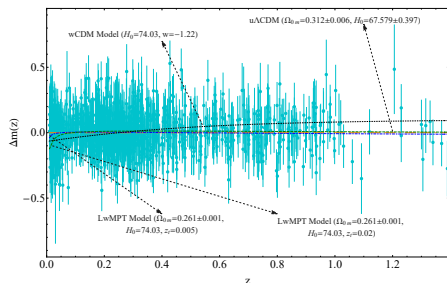
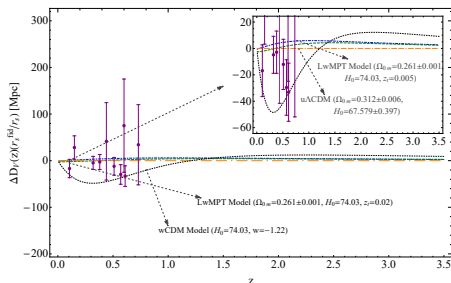
$$\chi^2 = \chi_{CMB}^2 + \chi_{BAO}^2 + \chi_{CC}^2 + \chi_{Panth}^2 \quad (12)$$

and calculate the residual $\Delta\chi^2$ with respect to the Λ CDM model for the *LwMPT* class (as a function of z_t) and for *wCDM* with $w = -1.22$ and $\omega_m \simeq 0.143$.



Fitting LwMPT to cosmological data

- We show the difficulty of the smooth $H(z)$ deformation models that address the Hubble tension in fitting the BAO and SNIa data. We show the BAO and SNIa data (residuals from the best fit Λ CDM) along with the best fit residuals for the w CDM and LwMPT models.



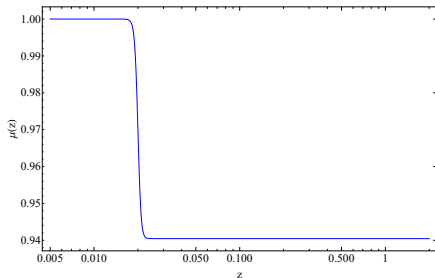
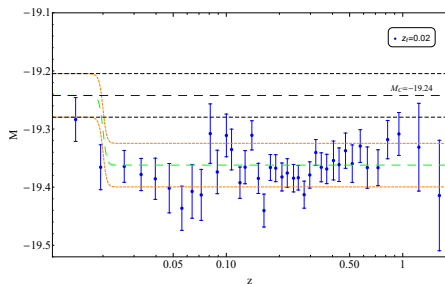
The M transition

- Assuming that the SNIa absolute luminosity is proportional to the Chandrasekhar mass which varies as $L \sim G_{\text{eff}}^b$ with $b = -3/2$ we obtain the required evolution of an effective Newton's constant that is required to produce the M transition. This assumption leads to the variation of the SNIa absolute magnitude M with $\mu \equiv \frac{G_{\text{eff}}}{G_{\text{N}}}$ (G_{N} is the locally measured Newton's constant)

$$\Delta M = \frac{15}{4} \log_{10} (\mu) \quad (13)$$

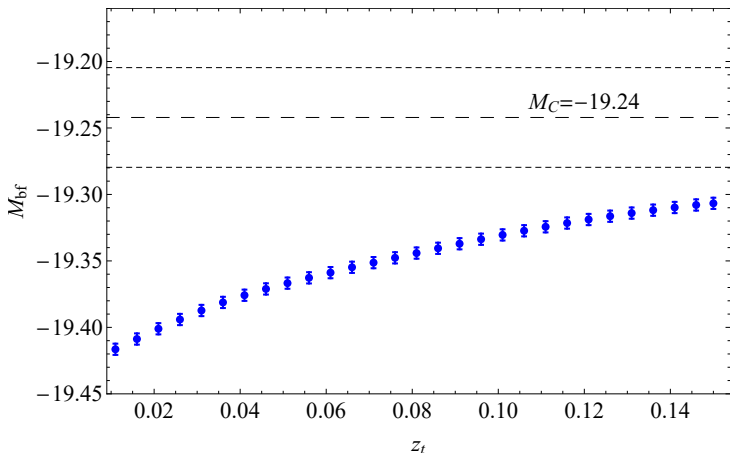
The M transition

- The form of the M transition that is necessary for LwMPT to be consistent with the Cepheid absolute magnitude, and the $\mu = G_{\text{eff}}/G_{\text{N}}$ required to induce it are shown below.



The M transition

- We present the best fit absolute magnitude M_{bf} (blue points) for various z_t for the $LwMPT$ model. The dashed line corresponds to the fixed M_C value, while the dot dashed lines correspond its 1σ error.



Regarding the growth tension

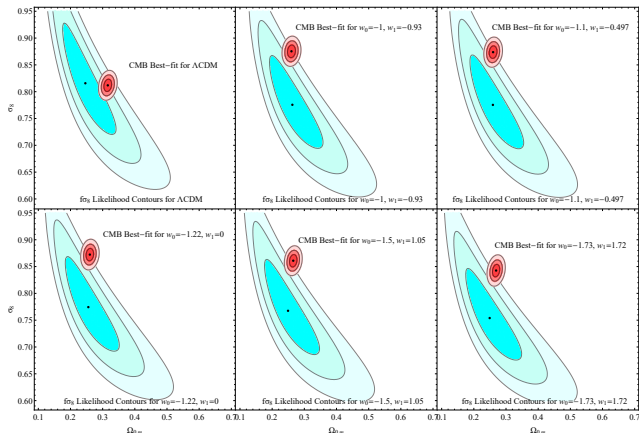
- We have demonstrated by using a generic CPL model that attempts to seemingly solve the H_0 tension that all parametrizations that use late time smooth deformations of the Hubble expansion rate $H(z)$ of the Planck18/ Λ CDM best fit, in order to match the locally measured value of H_0 while effectively keeping the comoving distance to the last scattering surface and $\Omega_{0m}h^2$ fixed to maintain consistency with Planck CMB measurements fail to address the growth tension.

Regarding the growth tension

- We have demonstrated by using a generic CPL model that attempts to seemingly solve the H_0 tension that all parametrizations that use late time smooth deformations of the Hubble expansion rate $H(z)$ of the Planck18/ Λ CDM best fit, in order to match the locally measured value of H_0 while effectively keeping the comoving distance to the last scattering surface and $\Omega_{0m}h^2$ fixed to maintain consistency with Planck CMB measurements fail to address the growth tension.
- In the case of CPL the fact that the tension does not ease is shown by the contours that correspond to the Growth and the Plank 18 CMB data, for the Λ CDM and various (w_0, w_1) pairs of the CPL model

Aleatas, G. and Perivolaropoulos, L., (2021), *Mon.Not.Roy.Astron.Soc.* 504 (2021) 3956

Regarding the growth tension



- However in the case of LwMPT we expect the growth tension to be improved or at least not be adversely impacted, since it does not fall in the category of smooth $H(z)$ deformations. Marra, Valerio and Perivolaropoulos, Leandros, (2021), arXiv:2102.06012 [astro-ph.CO]

The evolution of the Tully-Fisher data

- We use an up to date compilation of galaxy data to examine the evolution of the baryonic Tully-Fisher relation (BTFR).

The evolution of the Tully-Fisher data

- We use an up to date compilation of galaxy data to examine the evolution of the baryonic Tully-Fisher relation (BTFR).
- BTFR connects the total baryonic mass of a galaxy (M_B) with its rotation velocity,

$$M_B = A_B v_{rot}^s \quad (14)$$

where $\log(A_B)$ is the zero point or intercept in a logarithmic plot, and $s \simeq 4$ is the slope.

The evolution of the Tully-Fisher data

- We use an up to date compilation of galaxy data to examine the evolution of the baryonic Tully-Fisher relation (BTFR).
- BTFR connects the total baryonic mass of a galaxy (M_B) with its rotation velocity,

$$M_B = A_B v_{rot}^s \quad (14)$$

where $\log(A_B)$ is the zero point or intercept in a logarithmic plot, and $s \simeq 4$ is the slope.

- A tension in the evolution of BTFR could be attributed to a gravitational transition because,

$$A_B \sim G_{\text{eff}}^{-2} S^{-1} \quad (15)$$

where G_{eff} is the effective Newton's constant and S is the surface density.

The evolution of the Tully-Fisher data

- The logarithmic form of the BTFR is,

$$\log M_B = s \log v_{rot} + \log A_B \equiv s y + b \quad (16)$$

The evolution of the Tully-Fisher data

- The logarithmic form of the BTFR is,

$$\log M_B = s \log v_{rot} + \log A_B \equiv s y + b \quad (16)$$

- We can see that the intercept of the line is connected with the strength of the gravitational interactions.

The evolution of the Tully-Fisher data

- The logarithmic form of the BTFR is,

$$\log M_B = s \log v_{rot} + \log A_B \equiv s y + b \quad (16)$$

- We can see that the intercept of the line is connected with the strength of the gravitational interactions.
- While studies of the evolution of BTFR have been done in the past, none of them has focused at searching for abrupt transitions of the intercept or slope values at very low redshifts.

The evolution of the Tully-Fisher data

- The logarithmic form of the BTFR is,

$$\log M_B = s \log v_{rot} + \log A_B \equiv s y + b \quad (16)$$

- We can see that the intercept of the line is connected with the strength of the gravitational interactions.
- While studies of the evolution of BTFR have been done in the past, none of them has focused at searching for abrupt transitions of the intercept or slope values at very low redshifts.

That is exactly what we did. [Alestas G. et.al., \(2021\), arXiv:2104.14481 \[astro-ph.CO\]](#)

The evolution of the Tully-Fisher data

- We consider the BTFR dataset of the updated SPARC database consisting of the distance D , the logarithm of the baryonic mass $\log M_B$ and the logarithm of the asymptotically flat rotation velocity $\log v_{rot}$ of 118 galaxies along with their 1σ errors.

The main characteristics of our study is that,

The evolution of the Tully-Fisher data

- We consider the BTFR dataset of the updated SPARC database consisting of the distance D , the logarithm of the baryonic mass $\log M_B$ and the logarithm of the asymptotically flat rotation velocity $\log v_{rot}$ of 118 galaxies along with their 1σ errors.

The main characteristics of our study is that,

- We use an exclusively low z sample of data.

The evolution of the Tully-Fisher data

- We consider the BTFR dataset of the updated SPARC database consisting of the distance D , the logarithm of the baryonic mass $\log M_B$ and the logarithm of the asymptotically flat rotation velocity $\log v_{rot}$ of 118 galaxies along with their 1σ errors.

The main characteristics of our study is that,

- We use an exclusively low z sample of data.
- We focus on a particular type of evolution, sharp transitions of the intercept and slope.

The evolution of the Tully-Fisher data

- We fix a critical distance D_c and split our sample in two subsamples Σ_1 (galaxies with $D < D_c$) and Σ_2 (galaxies with $D > D_c$).

The evolution of the Tully-Fisher data

- We fix a critical distance D_c and split our sample in two subsamples Σ_1 (galaxies with $D < D_c$) and Σ_2 (galaxies with $D > D_c$).
- For each subsample we use the maximum likelihood method and perform a linear fit to the data setting $y_i = \log(M_B)_i$, $x_i = \log(v_{rot})_i$ while the parameters to fit are the slope and the intercept.

The evolution of the Tully-Fisher data

- We fix a critical distance D_c and split our sample in two subsamples Σ_1 (galaxies with $D < D_c$) and Σ_2 (galaxies with $D > D_c$).
- For each subsample we use the maximum likelihood method and perform a linear fit to the data setting $y_i = \log(M_B)_i$, $x_i = \log(v_{rot})_i$ while the parameters to fit are the slope and the intercept.
- Therefore, for each sample j ($j = 0, 1, 2$ with $j = 0$ corresponding to the full sample and $j = 1, 2$ corresponding to the two subsamples Σ_1 and Σ_2) we attempt to minimize,

$$\chi_j^2(s, b) = \sum_{i=1}^{N_j} \frac{[y_i - (s_j x_i + b_j)]^2}{s_j^2 + \sigma_{x_i}^2 + \sigma_{y_i}^2 + \sigma_s^2} \quad (17)$$

with respect to the slope s_j and intercept b_j .

The evolution of the Tully-Fisher data

- By demanding that $\frac{\chi_{0,min}^2}{N_0} = 1$ we fix the scatter to $\sigma_s = 0.077$, where $\chi_{0,min}^2$ is the minimized value of χ^2 for the full sample and N_0 is the number of data points of the full sample.

The evolution of the Tully-Fisher data

- By demanding that $\frac{\chi_{0,min}^2}{N_0} = 1$ we fix the scatter to $\sigma_s = 0.077$, where $\chi_{0,min}^2$ is the minimized value of χ^2 for the full sample and N_0 is the number of data points of the full sample.
- We thus find the best fit values of the parameters s_j and b_j , ($j = 0, 1, 2$).

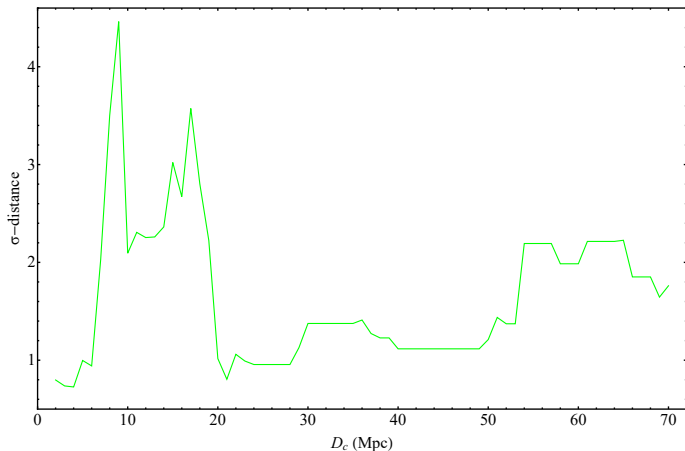
The evolution of the Tully-Fisher data

- By demanding that $\frac{\chi_{0,min}^2}{N_0} = 1$ we fix the scatter to $\sigma_s = 0.077$, where $\chi_{0,min}^2$ is the minimized value of χ^2 for the full sample and N_0 is the number of data points of the full sample.
- We thus find the best fit values of the parameters s_j and b_j , ($j = 0, 1, 2$).
- We then evaluate the $\Delta\chi_{kl}^2(D_c)$ of the best fit of each subsample k with respect to the likelihood contours of the other subsample l . Using these values we also evaluate the σ -distances ($d_{\sigma,kl}(D_c)$ and $d_{\sigma,lk}(D_c)$) and conservatively define the minimum of these σ -distances as,

$$d_{\sigma}(D_c) \equiv \text{Min} [d_{\sigma,12}(D_c), d_{\sigma,21}(D_c)] \quad (18)$$

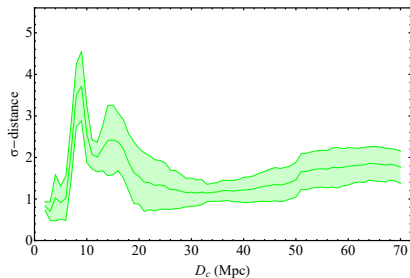
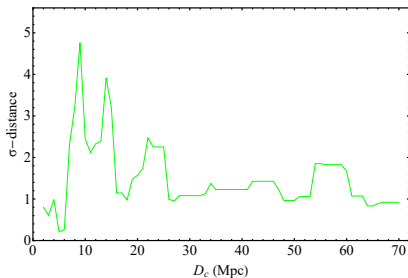
The evolution of the Tully-Fisher data

Plotting the σ -distance between the each pair of subsamples as a function of the split distance D_c we observe two statistically significant abrupt peaks at 9Mpc and 17Mpc .



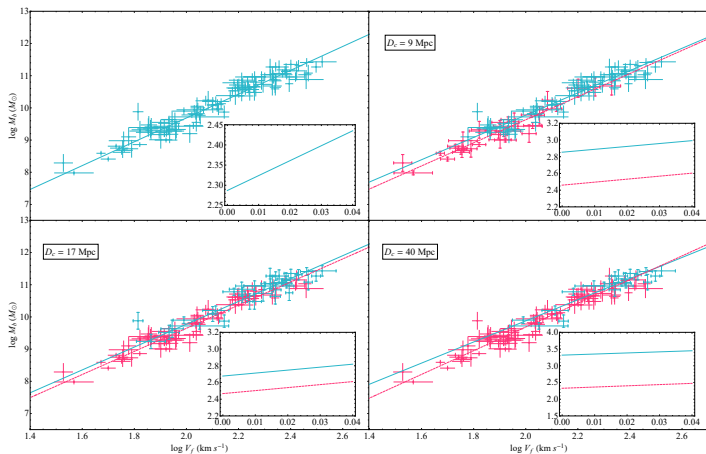
The evolution of the Tully-Fisher data

In order to make sure that our results are not biased due to not taking into account the uncertainties in the galactic distances we have repeated the analysis using Monte Carlo simulations of 100 samples with randomly varying galaxy distances. The distance to each galaxy in each random sample varied randomly with a Gaussian distribution with mean equal to the measured distance and standard deviation equal to the corresponding 1σ error. The results of this analysis are shown in the following figure,



The evolution of the Tully-Fisher data

These are the best fit $\log M_B - \log v_{rot}$ lines for selected galactic subsamples superimposed with the datapoints. The difference between the two lines for $D_c = 9\text{Mpc}$ and $D_c = 17\text{Mpc}$ is evident even though their slopes are very similar.



Summary

- We have stated the true problem in the heart of the Hubble tension. The fact that it concerns first and out foremost the absolute magnitude.

Summary

- We have stated the true problem in the heart of the Hubble tension. The fact that it concerns first and out foremost the absolute magnitude.
- We have demonstrated how, at least in principle, a late time transition model could provide a resolution to the Hubble crisis. This model constitutes of a transition in the dark energy equation of state w coupled with a gravitational transition which is translated to an absolute magnitude M transition.

Summary

- We have stated the true problem in the heart of the Hubble tension. The fact that it concerns first and out foremost the absolute magnitude.
- We have demonstrated how, at least in principle, a late time transition model could provide a resolution to the Hubble crisis. This model constitutes of a transition in the dark energy equation of state w coupled with a gravitational transition which is translated to an absolute magnitude M transition.
- We have also given observational evidence supporting a such gravitational transition, in the form of a tension in the evolution of the baryonic Tully-Fisher relation. This tension seems to be of high statistical significance $3 - 4\sigma$, the anticipated magnitude but at a little lower redshift.

Looking Ahead

- The SH0ES measurement must be put under intense scrutiny, in case of systematic errors that elude us so far.

Looking Ahead

- The SH0ES measurement must be put under intense scrutiny, in case of systematic errors that elude us so far.
- The LwMPT model must be put under test using the full Planck likelihood data, not just the CMB shift parameters, and be compared with other parametrizations that make similar claims. This work is currently under way and the results for LwMPT are very promising.

Looking Ahead

- The SH0ES measurement must be put under intense scrutiny, in case of systematic errors that elude us so far.
- The LwMPT model must be put under test using the full Planck likelihood data, not just the CMB shift parameters, and be compared with other parametrizations that make similar claims. This work is currently under way and the results for LwMPT are very promising.
- Other astrophysical relations that involve gravitational physics like the Faber-Jackson relation between intrinsic luminosity and velocity dispersion of elliptical galaxies or the Cepheid star period-luminosity relation could also be screened for similar types of transitions as in the case of BTFR.

Thank you for listening!!

THE GRAVITATIONAL CONSTANT MIGHT NOT BE SO CONSTANT...



“This research is co-financed by Greece and the European Union (European Social Fund-ESF) through the Operational Programme «Human Resources Development, Education and Lifelong Learning 2014- 2020» in the context of the project “Scalar fields in Curved Spacetimes: Soliton Solutions, Observational Results and Gravitational Waves” (MIS 5047648).”



Operational Programme
Human Resources Development,
Education and Lifelong Learning

Co-financed by Greece and the European Union



Guest Stars!